Perspective

Challenges for the modern analytical ultracentrifuge analysis of polysaccharides

Stephen E. Harding*

NCMH Physical Biochemistry Laboratory, University of Nottingham, School of Biosciences, Sutton Bonington LE12 5RD, UK

Dedicated to Professor David Brant

Abstract—This article reviews some of the recent advances in analytical ultracentrifugation and how these advances have impacted—and can impact—on our understanding of the size, shape through conformation modelling, interactions and charge properties of polysaccharides in solution, particularly when used in combination with other solution techniques and also imaging techniques. Specifically we look at (1) polysaccharide polydispersity and simple shape analysis by sedimentation velocity, and in particular using new approaches such as SEDFIT analysis; (2) polysaccharide molecular-weight analysis by sedimentation equilibrium and MSTAR analysis and how this complements analysis of size exclusion chromatography coupled to multi-angle laser light scattering; (3) polysaccharide conformation analysis using traditional procedures such as the Wales–van Holde ratio, power law or 'scaling' relations, more specialised treatments for rigid cylindrical structures, semi-flexible chains and worm-like coils and complications through draining effects; (4) Analysis of polysaccharide interactions and in particular complex formation phenomena, focusing on interesting applications in the areas of mucoadhesion and sedimentation fingerprinting; and (5) the possibilities for macromolecular charge and charge screening measurement.
© 2005 Elsevier Ltd. All rights reserved.

Keywords: Conformation; Interaction; Velocity; Equilibrium; SEDFIT; MSTAR

1. Introduction

The last two decades have seen significant advances in analytical ultracentrifugation for the analysis of molecular weight, oligomeric state, solution conformation and interactions of macromolecules. Much of the attention has focussed on proteins, protein–protein and protein–ligand interactions[1,2] but there are now many new possibilities for polysaccharide analysis. The ultracentrifuge is, of course, only one of a suite of methods for obtaining fundamental biophysical information about solutions of polysaccharides, but as is well known, these substances are by no means easy to characterise. These difficulties arise from their highly expanded nature in solution, their polydispersity, the large variety of confor-

mation and in many cases their high charge.[3,4] All of these features can complicate considerably the interpretation of solution data but nonetheless provide a fascinating challenge to the biophysical chemist—and the ultracentrifuge. The analytical ultracentrifuge is well positioned to deal with this mainly because of its diversity, its absolute nature and inherent fractionation ability and without the need for separation columns or membranes.[5] As with other methods it is of course most powerful when it is used in combination with other solution techniques, and, where appropriate, with imaging techniques like electron microscopy and atomic force microscopy. In this way data from the ultracentrifuge can provide the basis for some powerful modelling of the overall conformation and flexibility of polysaccharides in solution, complementing approaches such as those of David Brant and co-workers who have been at the forefront of investigating the local spatial

* Tel.: +44 9516148; fax: +44 95161452; e-mail: steve.harding@nottingham.ac.uk

distribution and dynamic properties of polysaccharides using NMR, X-ray scattering and atomic force microscopy as the basis of such modelling.[6–11]

This article highlights some of the key advances and challenges in the following areas: (1) Polysaccharide polydispersity and simple shape analysis by sedimentation velocity, and in particular using new approaches such as SEDFIT analysis which take advantage of the automatic data capture and analyses facilities of the new generation XL-I analytical ultracentrifuge; (2) polysaccharide molecular-weight analysis by sedimentation equilibrium focussing on model-independent procedures such as MSTAR, and how these procedures complement analysis of size exclusion chromatography coupled to multi-angle laser light scattering; (3) polysaccharide conformation analysis using traditional procedures such as the Wales–van Holde ratio, power law or 'scaling' relations, more specialised treatments for rigid cylindrical structures, semi-flexible chains and worm-like coils and complications through draining effects; (4) analysis of polysaccharide interactions and in particular complex formation phenomena, involving interesting applications in the areas of mucoadhesion and sedimentation fingerprinting and (5) finally we look at the possibilities for macromolecular charge and charge screening measurement.

2. Recording concentration distributions in the analytical ultracentrifuge

Although some of the older-generation Beckman Model E and MOM ultracentrifuges are still in use, the principal instrument for the analytical ultracentrifugation of polysaccharide solutions since its launch in 1996 has been the Optima XL-I from Beckman Instruments (Palo Alto, USA).[12] The laser (wavelength 670 nm) on this instrument provides high-intensity, highly collimated light and the resulting interference patterns (formed between light passing through the solution and the reference solvent sectors of an ultracentrifuge cell) are captured by a CCD camera. A Fourier transformation converts the interference fringes into a record of concentration $c(r) - c(a)$ relative to the meniscus ($r = a$) as a function of radial displacement r from the axis of rotation. The measurement is in terms of Rayleigh fringe units relative to the meniscus, $j(r)$, with $J(r) = j(r) + J(a)$, $J(r)$ being the absolute fringe displacement and $J(a)$ the absolute fringe displacement at the meniscus. For a standard optical path-length cell ($l = 1.2$ cm) with laser wavelength $\lambda = 6.70 \times 10^{-5}$ cm, a simple conversion exists from $j(r)$ in fringe displacement units to $c(r)$ in g/mL:

$$c(r) = J(r)\lambda / \{(\mathrm{d}n/\mathrm{d}c)l\}$$
$$= \{5.58 \times 10^{-5}/(\mathrm{d}n/\mathrm{d}c)\} \cdot j(r) \qquad (1)$$

with similar conversions for $J(a)$ to $c(a)$ and $j(r)$ to $c(r) - c(a)$. The term $\mathrm{d}n/\mathrm{d}c$ is the (specific) refractive index increment, which depends on the polysaccharide, solvent and wavelength. A comprehensive list of values for a range of macromolecules has recently been published.[13] In aqueous systems most values lie between 0.14 and 0.16 mL/g, although for nonaqueous systems the values can range enormously (from 0.044 to 0.218 mL/g). For example, the data for κ-carrageenan[13] suggest little temperature dependence, whilst that for dextrans suggests a significant dependence on wavelength. A study on the polycationic chitosan[14] suggested that the degree of substitution of some polysaccharides can strongly affect $\mathrm{d}n/\mathrm{d}c$, particularly if ionic groups are involved. Preston and Wik[15] have explored in detail the effect of ionic strength and wavelength on $\mathrm{d}n/\mathrm{d}c$ for the polyanion hyaluronate. These results show that if a user needs, for whatever reason, an accurate value for $\mathrm{d}n/\mathrm{d}c$ for a polysaccharide he should measure it directly in the particular buffer used for the ultracentrifuge experiments.

At this point it is worth stressing that converting fringe concentrations $\{j(r)$ or $J(r)\}$ to weight concentrations is normally not necessary for most applications. In addition, for sedimentation velocity work it is possible to work with $j(r)$ or $c(r) - c(a)$, namely, concentrations relative to the meniscus, without having to worry about measuring the offset or meniscus concentration $J(a)$ or $c(a)$ to convert to absolute $J(r)$ or $c(r)$.

3. Polysaccharide polydispersity and simple shape analysis by sedimentation velocity

With sedimentation velocity we measure the change in solute distribution across a solution in an ultracentrifuge cell as a function of time. Traditional analysis methods on these measurements have been based around recording the movement of the radial position of the boundary r_b with time t, from which a sedimentation coefficient, s (sec or Svedbergs, S, where $1\,\mathrm{S} = 10^{-13}$ sec) can be obtained:[16]

$$s = (\mathrm{d}r_b/\mathrm{d}t)\omega^2 r_b \qquad (2)$$

ω is the angular velocity (rad/s). Since the measured s will be affected by the temperature, density and viscosity of the solvent in which it is dissolved it is usual to normalise to standard conditions—namely the density and viscosity of water at 20.0 °C to yield $s_{20,w}$[16]

$$s_{20,w} = \{(1 - \bar{v}\rho_{20,w})/(1 - \bar{v}\rho_o)\} \cdot \{\eta_o/\eta_{20,w}\} \cdot s_{T,b} \qquad (3)$$

ρ_o and η_o are the densities and viscosities of the buffer, $\rho_{20,w}$ and $\eta_{20,w}$ the corresponding values at 20.0 °C in water. $\bar{v}$ is the partial specific volume, which for neutral polysaccharides can often be reasonably estimated from

the carbohydrate content[17] and takes on values between 0.5 and 0.7 mL/g for neutral polysaccharides in aqueous solvent. In cases where estimates based on composition cannot be reasonably made—such as for polyanionic and polycationic materials—$\bar{v}$ can be measured by densimetry[18] coupled with accurate concentration measurement. For example Preston and Wik[15] have shown that $\bar{v}$ for hyaluronan varies from 0.47 to 0.57 from ionic strengths 0.001–0.25 mol L^{-1}. A computer algorithm SEDNTERP[19,20] has been developed for facilitating the correction in Eq. 3. There is no longer any need (except for unusual solvents) to look up solvent densities and viscosities in the Chemical Rubber Handbook or other data books—a user of the algorithm just has to specify the buffer composition and the temperature of the measurement and the correction is done automatically.

The s and $s_{20,w}$ obtained from Eqs. 1–3 will be *apparent* values because of the effects of solution nonideality, deriving from co-exclusion and—for charged polysaccharides—polyelectrolyte effects.[16] To eliminate the effects of nonideality it is necessary to measure either s or $s_{20,w}$ for a range of different cell-loading concentrations c, and perform an extrapolation to zero concentration. For polysaccharides this has been conventionally achieved from a plot of $1/s$ (or $1/s_{20,w}$) versus c:[16]

$$\{1/s\} = \{1/s^o\} \cdot \{1 + k_s c\} \tag{4}$$

a relation valid over a limited range of concentration. k_s is the Gralén coefficient named after Svedberg's doctoral student who introduced this term in his 1944 thesis on the analysis of cellulose and its derivatives.[21]

For a wider span of concentrations, a more comprehensive description of concentration dependence has been given by Rowe:[22,23]

$$s = s^o\{1 - [k_s c - (((c v_s)^2(2\phi_p - 1))/\phi_p^2)]/[k_s c - 2c v_s + 1]\} \tag{5}$$

v_s (mL/g) is the 'swollen' specific volume of the solute (volume (mL) of a polysaccharide swollen through solvent association per gram of the anhydrous molecule) and ϕ_p is the maximum packing fraction of the solute ($\sim$0.4 for biological solutes[23]). A least-squares proFit (Quantum Soft, Zurich, Switzerland) algorithm has been developed for fitting s versus c data to Eq. 5.

For a polydisperse solution—the hallmark of solutions of polysaccharides—s (and s^o) will be a weight average.[16,24,25] If the solution contains more than one discrete (macromolecular) species—such as a mixture of different polysaccharides, the polydispersity will be manifested by asymmetry in the sedimenting boundary or, if the species have significantly different values for $s_{20,w}$, discrete boundaries are resolved[26] as we will consider later in this article.

3.1. Sedimentation coefficient distributions: SEDFIT

Since the appearance of the new-generation analytical ultracentrifuges in 1990 (XL-A) and 1996 (XL-I), the acquisition of multiple on-line data acquisition has resulted in some important advances in software for recording and analysing not only the change in boundary position with time but the change in the whole radial concentration profile, $c(r,t)$ with time t. This advance has in particular facilitated the measurement of *distributions* of sedimentation coefficient.[27–30] The (differential) distribution of sedimentation coefficients can be defined as the population (weight fraction) of species with a sedimentation coefficient between s and $s + \mathrm{d}s$.[27] Different symbols have been given for this parameter, either $g(s)$ or $c(s)$ {the latter, of units weight concentration (g/ mL) per second or Svedberg, is not to be confused with the same symbol c conventionally used for weight concentration here and elsewhere in the ultracentrifuge literature}. A plot of $g(s)$ [or $c(s)$] versus s then defines the distribution. Integration of a peak or resolved peaks from these types of plot can then be used to calculate the weight average s of the sedimenting species and their partial loading concentrations.

The simplest way computationally of obtaining a sedimentation coefficient distribution is from time derivative analysis of the evolving concentration distribution profile across the cell.[27,28] More recently, attention has turned to direct modelling of the evolution of the concentration distribution with time for obtaining the sedimentation coefficient distribution.[29,30] The distribution has been related to the experimentally measured evolution of the concentration profiles throughout the cell by a Fredholm integral equation

$$a(r,t) = \int_{s\,\min}^{s\,\max} c(s) \cdot \chi(s,D,r,t)\,\mathrm{d}s + a_{\mathrm{TI}}(r) + a_{\mathrm{RI}}(t) + \varepsilon \tag{6}$$

In this relation $a(r,t)$ is the experimentally observed signal, ε represents random noise, $a_{\mathrm{TI}}(r)$ represents the time invariant systematic noise and $a_{\mathrm{RI}}(t)$ radial invariant systematic noise: Schuck[29] and Dam and Schuck[30] described how this systematic noise is eliminated. χ is the normalised concentration at r and t for a given sedimenting species of sedimentation coefficient s and translational diffusion coefficient D: it is normalised to the initial loading concentration so it is dimensionless. The evolution with time of the concentration profile $\chi(s,D,r,t)$ in a sector shaped ultracentrifuge cell is given by the Lamm[31] equation:

$$\frac{\partial \chi}{\partial t} = (1/r) \cdot \frac{\partial}{\partial r}\left[rD\frac{\partial \chi}{\partial r} - s\omega^2 r^2 \chi \right] \tag{7}$$

Although only approximate analytical solutions to this partial differential equation have been available for $\chi(s,D,r,t)$, accurate numerical solutions are now possible using finite element methods first introduced by Claverie et al.[32] and recently generalised to permit greater efficiency and stability:[29,30] the algorithm SEDFIT[33] employs this procedure for obtaining the sedimentation coefficient distribution. To solve Eq. 6 to obtain $c(s)$ as a function of s requires s_{min} and s_{max} to be carefully chosen and adjusted accordingly: inappropriate choice can be diagnosed by an increase of $c(s)$ towards the limits of s_{min} or s_{max}. However the contribution from diffusion broadening also has to be dealt with. SEDFIT offers two ways. The first is using a dependence of D on s, via the translational frictional ratio f/f_o:

$$D(s) = \{(\sqrt{2})/(18\pi)\} \cdot k_B t \cdot s^{-1/2}(\eta_o(f/f_o)_w)^{-3/2}((1 - \bar{v}\rho_o)/\bar{v})^{-1/2} \tag{8}$$

f is the frictional coefficient of a species and f_o the corresponding value for a spherical particle of the same mass and (anhydrous) volume (see e.g., Ref. 34). k_B is the Boltzmann constant. Although of course a distribution of s implies also a distribution in D and f/f_o, for protein work advantage is taken of the fact that the frictional ratio is a relatively insensitive function of concentration: a single or weight average f/f_o is taken to be representative of the distribution. Using this assumption, Eq. 6 can be numerically inverted—that is, solved—to give the sedimentation coefficient distribution, with the position and shape of the $c(s)$ peak(s) more representative of a true distribution of sedimentation coefficient. $(f/f_o)_w$, where the subscript w denotes a weight average, is determined iteratively by nonlinear regression, optimising the quality of the fit of the $c(s)$ as a function of $(f/f_o)_w$. It has been shown by extensive simulation that non-optimal values of $(f/f_o)_w$ have little effect on the position of the $c(s)$ peaks, although they affect the width and resolution, i.e. the correct s value is reported. Regularisation[33] can be used, which provides a measure of the quality of fit from the data analysis. The assumption of a single f/f_o representing the whole macromolecular distribution may be reasonable for proteins but it is open to question whether this is so for polysaccharides. The inappropriateness of this assumption will affect the reliability of distribution widths, but not peaks. Better approximations are being investigated.

The current version of SEDFIT also offers the option of evaluating the distribution corresponding to nondiffusing particles, viz $D \sim 0$, that is, the diffusive contribution to Eq. 6 is small compared to the sedimentation contribution. In this case, Eq. 6 can be inverted without any assumptions concerning f/f_o. If diffusive effects are significant it will be an apparent sedimentation coefficient distribution, given as $g^*(s)$ versus s and the correct s value for a peak is still reported. Figure 1 gives a com-
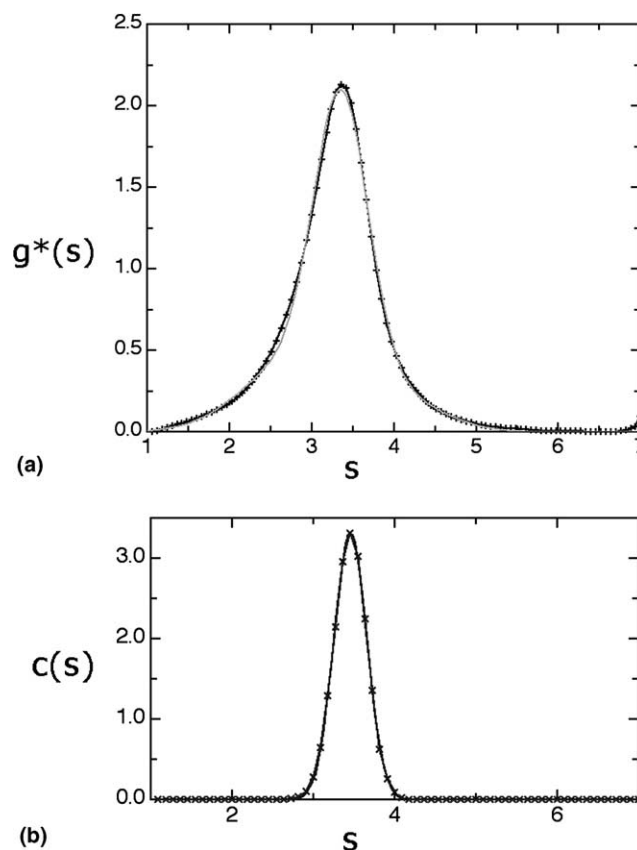

Figure 1. Sedimentation concentration distribution plots for guar gum using SEDFIT. (a) $g^*(s)$ versus s, (b) $c(s)$ versus s. A Gaussian fit to the data (lighter line) is also shown in (a). Rotor speed was 40,000 rpm at 20.0 °C, concentration was 0.75 mg/mL in 0.02% NaN_3. The guar suspension had been heated at 160 °C for 10 min at a pressure of 3 bar. From Ref. 35.

parison of the least squares $g^*(s)$ versus s and $c(s)$ versus s distribution for guar gum.[35]

There is a clear shoulder on the low s (lower M) side of the $g^*(s)$ peak—consistent with some lower molecular weight material observed using the technique of SEC-MALLs (size-exclusion chromatography coupled to laser light scattering) whereas the $c(s)$ profile shows only a symmetric peak. The current $c(s)$ procedure in this instance seems to have 'oversmoothed' the data. We would suggest the evaluation of apparent distributions via $g^*(s)$ at present, particularly for slow-diffusing polysaccharides. Another example of a $g^*(s)$ plot where there has been clear separation of material of different molecular weight is shown in Figure 2 for starch.

It is possible to get molecular weight from the sedimentation coefficient if we assume a conformation or if we combine with other measurements, namely the translational diffusion coefficient via the Svedberg equation[36]

$$M = RT \cdot \{s^o/D^o\}/(1 - \bar{v}\rho_o) \tag{9}$$

where ρ_o is the solvent density (if s and D are their normalised values $s^o_{20,w}$, $D^o_{20,w}$ and ρ_o will be the density of water at 20.0 °C, 0.9981 g/mL). Eq. 9 has been popularly
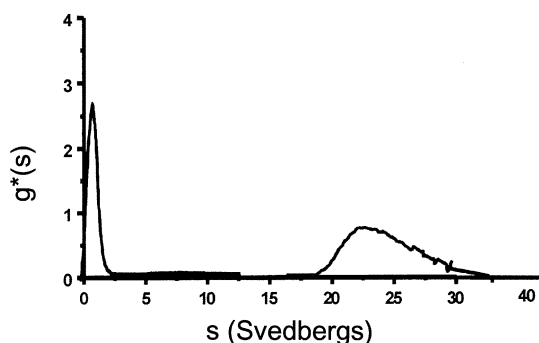
Figure 2. Sedimentation velocity $g*(s)$ profiles for starch polysaccharides. Wheat starch (containing amylose, left peak and the faster moving amylopectin, right peak), (total) sample concentration 8 mg/mL in 90% dimethyl sulfoxide. Rotor speed was 35,000 rpm at a temperature of 20 °C. From Ref. 26.
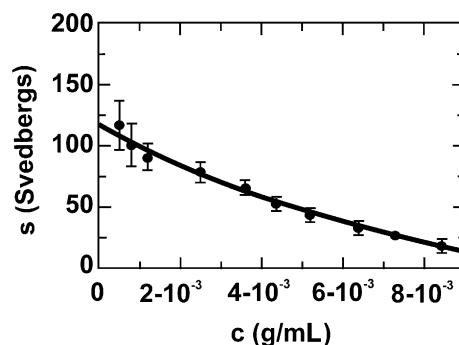

Figure 3. Concentration dependence of the sedimentation coefficient for wheat amylopectin. The data have been fitted to Eq. 5 (see text) yielding $s^o = (120 \pm 10)$ S, $k_s = (170 \pm 60)$ mL/g and $v_s = (40 \pm 4)$ mL/g. From Ref. 26.

used, for example, to investigate the molecular weights of carboxymethylchitins,[37,38] glycodendrimers,[40,41] galactomannans,[42] beta-glucans[43,44] and alginates.[45] The translational diffusion coefficient in Eq. 9 can in principle be measured from boundary spreading as manifested, for example, in the width of the $g*(s)$ profiles: although for monodisperse proteins this works well, for polysaccharides interpretation is seriously complicated by broadening through polydispersity. Instead special cells can be used, which allow for the formation of an artificial boundary whose diffusion can be recorded with time at low speed (~3000 rev/min). This procedure has been successfully employed, for example, in a recent study on heparin fractions.[46] Dynamic light scattering has been used as a popular alternative, and a good demonstration of how this can be performed to give reliable D data has been given by Burchard.[39] Whereas the s^o is a weight average, the value returned from dynamic light scattering for D^o is a z-average. As shown by Pusey,[47] combination of the two via the Svedberg equation (9) yields the weight average molecular weight, M_w although it is not clear what type of average for M is returned if an estimate for D^o is made from ultracentrifuge measurements.

Another useful combination that has been suggested is $s^o_{20,w}$ with k_s[22,23]

$$M_w = N_A \left[6\pi\eta s^o_{20,w}/(1 - \bar{v}\rho_0) \right]^{3/2} [(3\bar{v}/4\pi)(k_s/2\bar{v}) - (v_s/\bar{v})]^{1/2} \quad (10)$$

s, k_s and v_s can be obtained from fitting s versus c data to Eq. 5. The method was originally developed for single solutes and where charge effects can be neglected (either because the macromolecular solute is uncharged, or because the double layer or polyelectrolyte behaviour has been 'compressed' by the addition of neutral salt). For quasi-continuous distributions, such as polysaccharides, one can apply Eqs. 5 and 10 to the data, provided that for every concentration one has a 'boundary' to which a

weight-averaged s value can be assigned. If the plot of $1/s$ versus c is essentially linear over the data range, then specific interaction can be excluded, the solute system treated as a simple mixture and Eqs. 5 and 10 can be applied.

Figure 3 shows an example for wheat starch amylopectin, where concentrations for total starch have been normalised to amylopectin from the relative areas under the $g*(s)$ peaks. From this data a value for M_w of $\sim 30 \times 10^6$ g/mol is estimated.[26]

This equation is only approximate—any contributions from molecular charge to the concentration-dependence parameter k_s are assumed to be negligible or suppressed—but is nonetheless very useful when other methods—especially for very large polysaccharides like amylopectin—are inapplicable. For the latter case, this substance is too large for conventional sedimentation equilibrium determinations of molecular weight and solutions usually contain significant amounts of amylose: unlike sedimentation velocity, sedimentation equilibrium will not resolve away this component but contribute towards a total average molecular weight. Static light-scattering procedures based on the Rayleigh–Gans–Debye approximation are also compromised by the large size of amylopectin. These restrictions are not a problem for sedimentation velocity and the application of Eq. 10, which can also provide an estimate for the swollen specific volume v_s: for example, Majzoobi has obtained a value of (40 ± 4) mL/g for wheat starch amylopectin.[26]

For such polydisperse materials as polysaccharides, the question is what sort of average M value is yielded by doing so? In the absence of any obvious analytical solution, computer simulation has been used to determine the form of the average. In work to be published, A. J. Rowe and co-workers have shown that even for 'unfavourable' simulated mixtures (e.g., multi-modal, no central tendency), the average M value yielded is very close to an M_w (i.e., weight-averaged M). To put this in quantitative terms, the departure from M_w is generally <1% of the way towards M_z. This is trivial, in terms of the errors present in the raw data. Thus, there is an

exact procedure which can be defined for the evaluation of M (average) in a polydisperse solute system under the defined conditions, and simulation demonstrates that for all practical purposes the outcome is an M_w.

A sedimentation coefficient *distribution*—either $c(s)$ versus s or $g^*(s)$ versus s—for a polysaccharide can also be converted into an apparent molecular-weight distribution if the conformation of the polysaccharide is known or can be assumed, via a power law or 'scaling' relation:

$$s_{20,w}^o = K''M^b \qquad (11)$$

where the power law exponent is dependent on the conformation of the macromolecule, with the limits, in the case of nondraining molecules $b \sim 0.15$ for a rigid rod and ~ 0.67 for a compact sphere. A flexible coil shape molecule has a $b \sim 0.4$–0.5.[48,49] An early example of this transformation has been given for a heavily glycosylated mucin glycoprotein with polysaccharide-like properties[50] based on a $g^*(s)$ versus s distribution given by Pain.[51] The assumption was made that the contribution from diffusion broadening of these large molecules was negligible in comparison to sedimentation. Incorporation of Eq. 11 instead of Eq. 8 into the $c(s)$ versus s evaluation process is now being considered for polysaccharides.

4. Polysaccharide molecular-weight analysis, MSTAR, and the new role for sedimentation equilibrium

Whereas in a sedimentation velocity experiment at relatively high rotor speed—for a polysaccharide say 40,000–50,000 rev/min—the sedimentation rate and hence sedimentation coefficient are a measure of the size and shape of the molecule, at much lower speeds, say 10,000 rev/min or less in a sedimentation equilibrium experiment, the forces of sedimentation and diffusion on the macromolecule become comparable and instead of producing a sedimenting boundary, a steady-state equilibrium distribution of macromolecule is attained with a low concentration at the air/solution meniscus building up to a high concentration at the cell base. This final steady-state pattern[52] is a function only of molecular weight and related parameters (nonideal virial coefficients and association constants were appropriate) and not on molecular shape since at equilibrium there is no net transport or frictional effects: sedimentation equilibrium in the analytical ultracentrifuge is an absolute way of estimating molecular weight.

However, although the procedure is reliable, when done properly it is quite slow and the method of choice for obtaining polysaccharide molecular weights in solution is now SEC-MALLs (size exclusion chromatography coupled to laser light scattering): see, for example, Refs. 53–58. Nonetheless uncertainties can sometimes remain, particularly if materials have been incompletely clarified or there are problems with the columns (the

form of the angular dependence data can usually tell us if things are not well). Sedimentation equilibrium offers a powerful and valuable independent check on the results generated from SEC-MALLs: although it takes a longer time to generate a result, and molecular-weight distributions are considerably more difficult to obtain, agreement of M_w from sedimentation equilibrium with M_w from SEC-MALLs gives the researcher increased confidence in some of the other information (molecular-weight distribution and R_g–M dependence) coming from the latter.

Since polysaccharides are by their very nature polydisperse, the value obtained from sedimentation equilibrium will be an average of some sort. With Rayleigh interference and, where appropriate, UV-absorption optics, the principal average obtained is the weight average, M_w.[16] Although relations are available for obtaining number average M_n and z-average M_z data these latter averages are difficult to obtain with any reliable precision. Direct recording of the concentration gradient dc/dr versus radial displacement r using refractive index gradient or 'Schlieren' optics however facilitates the measurement of M_z (see Ref. 59). Such an optical system is unfortunately not present on the present generation XL_A or XL-I ultracentrifuges except for in-house adapted preparative XL ultracentrifuges.[60] Schlieren optics are also present on the older generation Model E analytical ultracentrifuge: this is one of the main reasons why we at the NCMH have kept and maintained one of these instruments.

An important consideration with polysaccharides is that at sedimentation equilibrium there will be a redistribution not only of total concentration of polysaccharide throughout the cell (low concentration at the meniscus building up to a higher concentration at the cell base) but also a redistribution of species of different molecular weight, with a greater proportion of the higher molecular weight part of the distribution appearing near the cell base. In obtaining a true weight (or number, z averages) it is therefore important to consider the *complete* concentration distribution profile throughout the ultracentrifuge cell, a feature often missed by some researchers. The problem can be minimised by the use of ultra-short solution columns ($\sim$0.7 mm from cell meniscus to base as opposed to the conventional 2–3 mm) leading to reduced redistribution material (see e.g., Ref. 61) but at the price of considerably reduced precision.

A procedure known as MSTAR—which can now run from a Windows rather than MSDOS platform—takes into account the full distribution and without requirement of very short columns. We will outline this briefly, although for clarity we will confine our consideration only to the extraction of the two most directly related parameters: the weight average molecular weight and the molecular-weight distribution. The extraction of other less useful parameters are avoided here but can be found in other articles (see Refs. 62–65).

As already stated, UV-absorption optics—when they can be applied—have the advantage that the recorded absorbances $A(r)$ as a function of radial position are (within the Lambert Beer law limit of $A(r) \sim 1.4$) directly proportional to the weight concentration $c(r)$ in g/mL. Although the multiple fringes in interference optics give a much more precise record of concentration, we stress again, these are *concentrations relative to the meniscus*, that is, we obtain directly from the optical records a profile of $c(r) - c(a)$ versus radial displacement r, with the meniscus at $r = a$. In fringe displacement units this is $J(r) - J(a)$, which we write as $j(r)$ for short. To obtain molecular-weight information we need $J(r)$ and hence some way of obtaining $J(a)$ is required: this is not such a requirement for sedimentation velocity where relative concentrations are sufficient. The polydisperse nature of polysaccharide prohibits the use of meniscus depletion methods (as by selecting a high enough speed so that $J(a) \sim 0$) because of loss of optical registration near the cell base. Furthermore, it was recently shown by Hall et al.[66] that simply floating it as another variable in the procedure for extracting M_w is not valid, particularly for polydisperse or interacting systems. A convenient procedure for extracting $J(a)$ and then M_w was given by Creeth and Harding over two decades ago:[67] a manipulation of the fundamental equation of sedimentation equilibrium leads to a function called $M^*(r)$ with dimensions of molar mass at a radial position r and is defined by

$$M^*(r) = j(r)/\left\{ kJ(a)(r^2 - a^2) + 2k \int_a^r r \cdot j(r)\, dr \right\}$$

(12)

where $k = (1 - \bar{v}\rho_o)\omega^2/2RT$, with ρ_o the solvent density. Eq. 12 has the limiting form

$$\lim_{r \to a}\{j(r)/(r^2 - a^2)\} = k \cdot M^*(a) \cdot J(a)$$

(13)

A plot of $j(r)/(r^2 - a^2)$ versus $\{1/(r^2 - a^2)\}$. $\int_a^r r \cdot j(r)\, dr$ has a limiting slope of $2kM^*(a)$ and an intercept $kM^*(a) \cdot J(a)$. Hence $J(a)$ is determinable from $2 \times$ (intercept/limiting slope). Once $J(a)$ has been found M^* as a function of radial position r can be defined. Hall et al.[66] and the manual for MSTAR[68] describe a method involving synthetic boundary cell that can be used to reinforce the determination of $J(a)$ in this way.

A particularly useful property of the M^* function is that at the cell base ($r = b$),

$$M^*(b) = M_{w,app}$$

(14)

the apparent weight average molecular weight of the polysaccharide.[67] It will be an apparent value because it will be affected by thermodynamic nonideality (molecular co-exclusion and, for charged polysaccharides, polyelectrolyte behaviour), which needs to be corrected for (see below). Optical distortion effects at the cell base means that a short extrapolation of $M^*(r)$ to $M^*(=b)$ is required,
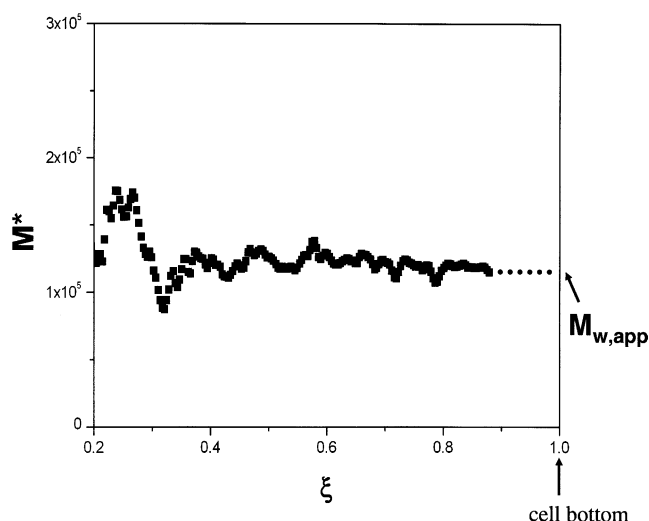

Figure 4. Sedimentation equilibrium MSTAR analysis of a chitosan. MSTAR analysis for $M_{w,app}$, from optical registration of the concentration distribution using Rayleigh interference optics on the XL-I ultracentrifuge and Eqs. 12 and 14 (see text) for chitosan G213. $M_{w,app} = 110{,}000$ g/mol. ξ is a normalised radial displacement squared parameter: $\xi = (r^2 - a^2)/(b^2 - a^2)$ where r is the radial displacement from the axis of rotation at a given point in the ultracentrifuge cell, and a and b the corresponding radial positions at the solution meniscus and cell base, respectively. $\xi = 0$ at the meniscus and $=1$ at the cell base. Loading concentration 1.0 mg/mL in 0.2 M acetate buffer. From Ref. 69.

but this normally poses no difficulty. Practical details behind the MSTAR algorithm upon which this procedure is based can be found from the Web download[68] and Refs. 64,65 and a recent example shown in Figure 4.[69]

It is worth pointing out here that another popular algorithm for analysing molecular weight from sedimentation equilibrium is *NONLIN*.[70] Whereas this is useful for the analysis of protein systems (monodisperse or associating), for polydisperse system like polysaccharides it is unsuitable: the estimate for $M_{w,app}$ obtained refers only to a selected region of the ultracentrifuge cell, and provides no rigorous procedure for dealing with the meniscus concentration problem.

4.1. Correcting for thermodynamic nonideality: obtaining M_w from $M_{w,app}$

For polysaccharides, nonideality, arising from co-exclusion volume and polyelectrolyte effects, can be a serious problem and, if not corrected for, can lead to significant underestimates for M_w: this was considered in detail in an earlier review.[62] It was possible with the older generation Model E ultracentrifuges—which could accommodate long (30 mm) optical path length cells—to work at very low solute loading concentrations (0.2 mg/mL). At these concentrations, for some polysaccharides—particularly neutral ones or those of molecular weight < 100,000—the nonideality effect could be neglected: the estimate for $M_{w,app}$ was within a few percent of

the true or 'ideal' M_w.[62] However the new generation XL-I can only accommodate a maximum 12 mm optical path-length cell with a minimum concentration requirement of 0.5 mg/mL: lower concentrations produce insufficient fringe displacement for meaningful analysis. This is another reason why we have kept running a Model E ultracentrifuge in the NCMH. This makes a large difference to the severity of the nonideality problem as Table 2 in Ref. [62] shows. The term $(1 + 2BM_{wc})$, where B is the thermodynamic second virial coefficient, represents the factor by which the apparent molecular weight measured at a finite concentration $c = 0.2$ mg/mL and 0.5 mg/mL underestimates the true or 'ideal' M_w. One can see that, whereas the earlier lower limit (0.2 mg/mL) for many cases led to only small errors for many cases, with the new instruments (limit 0.5 mg/mL) lead to severe underestimates in virtually all cases. Until there is an adaptation of the XL-I ultracentrifuge to enable the use of long path length cells, it is mandatory to measure $M_{w,app}$ over a range of loading concentrations followed by an extrapolation to zero concentration using an equation of the form[71]

$$\{1/M_{w,app}\} = \{1/M_w\} + 2Bc$$
$$= \{1/M_w\}(1 + 2BM_w c) \qquad (15)$$

correct to first order in concentration. The availability of four and eight-hole rotors in the XL-A and XL-I means that several concentrations can be run simultaneously. Further multiplexing is possible with the use of Yphantis style 6-channel ultracentrifuge cells,[72] which permit the simultaneous measurement of three solution/reference solvent pairs, although these tend to return $M_{w,app}$ values of lower accuracy. In some extreme cases, third or even higher virial coefficient(s) may be necessary to adequately represent the data: for example κ-carrageenan[73] and alginate.[74] In a recent study on alginates, Stratmann and Borchard[75] have demonstrated excellent agreement between M_w and B values obtained from sedimentation equilibrium and light-scattering methods.

4.2. Distributions of molecular weight

Direct interpretation of the sedimentation equilibrium concentration distribution profiles in terms of a molecular-weight distribution is generally impossible because of complications involving nonideality. Successful attempts have been given but only for simple discrete forms of polydispersity (two to three macromolecular species[76]). The simplest procedure for avoiding these complications[77] is to use sedimentation equilibrium in conjunction with gel-permeation chromatography (GPC). Fractions of relatively narrow (elution volume) bandwidth are isolated from the eluate and their M_w values evaluated by low-speed sedimentation equilibrium in the usual way: the GPC columns can thereby be 'self-cali-

brated' and elution volume values converted into corresponding molecular weights—a distribution can therefore be defined in a way which avoids the problem of using inappropriate standards for GPC: the value of multiplexing is clearly indicated. This procedure has been successfully applied to, for example, dextrans, alginates and pectins: for pectins excellent agreement with analogous procedures involving classical light scattering coupled to GPC has been obtained.[78]

5. Polysaccharide conformation analysis

The sedimentation coefficient s^o provides a useful indicator of polysaccharide conformation and flexibility in solution, particularly if the dependence of s^o on M_w is known.[49] There are two levels of approach: (i) a 'general' level in which we are delineating between overall conformation types (coil, rod, sphere), (ii) a more detailed representation where we are trying to specify particle dimensions in the case of rigid structures or persistence lengths for linear, flexible structures.

5.1. The Wales–van Holde ratio

The simplest indicator of conformation comes not from s^o but the sedimentation concentration dependence coefficient, k_s. Wales and Van Holde[79] were the first to show that the ratio of k_s to the intrinsic viscosity, $[\eta]$ was a measure of particle conformation. It was shown empirically by Creeth and Knight[80] that this has a value of ~1.6 for compact spheres and nondraining coils, and adopted lower values for more extended structures. Rowe[22,23] subsequently provided a derivation for rigid particles, a derivation later supported by Lavrenko et al.[81] The Rowe theory assumed there were no free-draining effects and also that the solvent had sufficient ionic strength to suppress any polyelectrolyte effects. A value of 1.6 was evaluated for spheres, reducing to ~0.2 for long rod-shape molecules.

Lavrenko et al.[81] also examined in detail the effects of free draining of solvent during macromolecular motion, demonstrating that this also had the effect of lowering $k_s/[\eta]$. A hydrodynamic intra-chain interaction or 'draining' parameter has been defined[82] with limits $X = \infty$ for the nonfree draining case and $X = 0$ for the free-draining case. A relation was given between $k_s/[\eta]$ and X:[81,82]

$$\{k_s/[\eta]\} = 8X/(3 + 8X) \qquad (16)$$

This relation evidently leads to theoretical limits for $k_s/[\eta] = 0$ for free draining and 1 for nonfree draining. The consequences of this are that unless the draining characteristics of the chain are properly known, one has to be cautious in making conclusions about particle asymmetry, since it has been claimed that draining affects can mimic increase in asymmetry in lowering the $k_s/[\eta]$. Notwithstanding, many nonspherical molecules have empiri-

cal values for $k_s/[\eta]$ greater than 1.0: pullulans for example, considered as a random coil have been shown to have $k_s/[\eta] \sim 1.4$ (see Ref. 83). Berth et al.[84] have argued that the very low $k_s/[\eta]$ values for chitosans are due to draining effects rather than a high degree of extension. Lavrenko et al.[81] have compiled an extensive list of $k_s/[\eta]$ values for a large number of other polysaccharides, complementing a list given by Creeth and Knight:[80] values are seen to range from 0.1 (potato amylose in 0.33 M KCl) to ~1.8 (a cellulose phenylcarbamate in 1,4-dioxane), with some polysaccharides showing a clear dependence on molecular weight.

5.2. Power law or 'scaling' relations

The relation linking the sedimentation coefficient with the molecular weight for a homologous polymer series given above is (see Ref. 48):

$$s = K''M^b \quad (11)$$

(n.b. Lavrenko et al.[81] call the exponent $1 - b$). This relation is similar to the well-known Mark–Houwink–Kuhn–Sakurada relation linking the intrinsic viscosity with molecular weight:

$$[\eta] = K'M^a \quad (17)$$

and also a relation linking the radius of gyration R_g with molecular weight.

$$R_g = K'''M^c \quad (18)$$

The power law or 'MHKS' exponents a, b, c have been related to conformation[48,49,85] (Table 1).

The coefficients in Table 1 correspond to the non-draining case. If draining effects are present then these will change the values for a and b—see, for example, Ref. 86. For example, it has been shown that a varies from 0.5 (nondraining case) to 1 (draining), again mimicking the effects of chain elongation. For homologous, linear types of polymer the power law indices are intercorrelated,[49] with

$$b \sim (1 - c), \quad a \sim (2 - 3b) \quad \text{and} \quad c \sim (a + 1)/3 \quad (19)$$

Another scaling relation exists between the sedimentation coefficient and k_s (see Ref. 81).

$$k_s = K''''(s^o)^{\text{æ}} \quad (20a)$$

Lavrenko et al. give æ and K'''' for a range of polysaccharides, and a similar relation linking the exponent æ with b:[81,49]

$$\text{æ} = (2 - 3b)/b \quad (20b)$$

Table 1. Power law exponents (from Ref. 48)

	a	b	c
Sphere	0	0.67	0.33
Coil	0.5–0.8	0.4–0.5	0.5–0.6
Rod	1.8	0.15	1.0

5.3. General conformation: Haug triangle and conformation zoning

Delineation of the three general conformation extremes (random coil, compact sphere, rigid rod) as indicated by the simple power or scaling laws and Wales/van Holde ratio, have been conveniently represented in the well-known Haug triangle (see Ref. 48). An extension of this idea was given by Pavlov et al.[87] who suggested the use of sedimentation coefficient s with the concentration dependence coefficient k_s and the mass per unit length M_L as a guide to the general conformation type or 'zone' of a polysaccharide. The zones were: A (extra rigid rod), B (almost rigid rod), C (semi-flexible coil), D (random coil), E (globular/branched). A and B are distinguished by B having a very limited amount of flexibility. The zones were constructed empirically using a large amount of data (s, k_s) accumulated for polysaccharides of 'known' conformation type, and plotted a scaling relation normalised with mass per unit length (M_L) measurements. The latter parameter can be obtained from knowledge of molecular weight from sedimentation equilibrium or light scattering and the chain length L from, small angle X-ray scattering, X-ray fibre diffraction or high resolution NMR: Pavlov and colleagues give a comprehensive comparison of methods for heparin.[46] If the molecular weight is known, M_L can also be estimated from electron microscopy.[88] Measurement of a data set (s, k_s, M_L) of any target polysaccharide would then establish its conformation type (Fig. 5). The limiting slopes of ~4 (extra rigid rod) and ~0 (globular/sphere) were shown to be theoretically reasonable. It should be
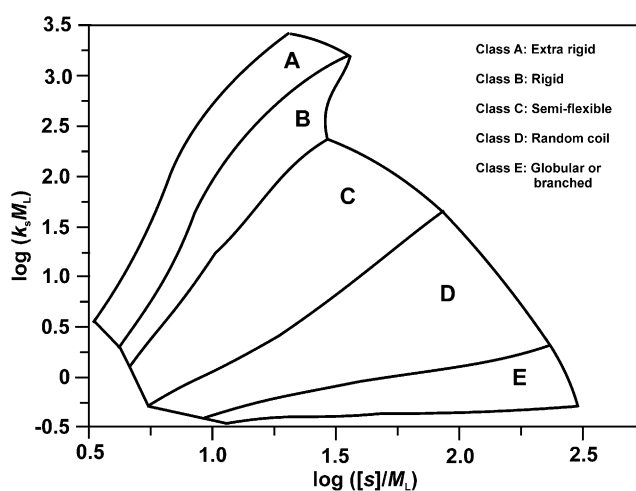
Figure 5. Conformation zoning of polysaccharide. Empirical plots for various polysaccharides of known conformation type. This helps to define zones: A: extra rigid rod, B: rigid rod, C: semi-flexible coil, D: random coil, E: globular/heavily branched structure. Measurement of s, k_s and M_L for a target polysaccharide then define its conformation zone or type. Redrawn and based on Ref. 87.

stressed that this procedure is only a guide to conformation type. Along with other procedures using k_s for conformation studies it assumes that charge contributions to the concentration have been suppressed by the supporting electrolyte, and also that draining effects are not significant or similar for the target polysaccharide and those polysaccharides whose data were used to set up the zones. Other normalised scaling relations have been suggested based on viscometry methods.[87]

5.4. Rigid cylindrical structures

Once a general conformation type or 'preliminary classification' has been established it is possible to use sedimentation data to obtain more detailed information about polysaccharide conformation. For example, the low value of $k_s/[\eta] \sim 0.25$ found for the bacterial polysaccharide xylinan has been considered to be due to asymmetry.[89] If we then assume a rigid structure, the approximate theory of Rowe[36,37] can be applied in terms of a prolate ellipsoid of revolution to estimate the aspect ratio $p(\sim L/d$ for a rod, where L is the rod length and d is its diameter) ~ 80.

For a cylindrical rod an expression also exists for the sedimentation coefficient:[90]

$$s^o = \{M(1 - \bar{v}\rho_o)/(3\pi\eta_o N_A L)\} \cdot \{\ln(L/d) + \gamma\} \quad (21)$$

where γ is a function of p and has a limiting value of ~ 0.386 for very long rods ($p \to \infty$). Replacing L by the (molar) mass per unit length $M_L = M/L$ (g mol^{-1} cm^{-1}) this becomes

$$s^o = \{M_L(1 - \bar{v}\rho_o)/(3\pi\eta_o N_A)\} \cdot \{\ln M - \ln M_L$$
$$- \ln d + \gamma\} \quad (22)$$

For the cases of finite p (in the range 2–20) the currently accepted expression for $\gamma(p)$ is that of Tirado and Garcia de la Torre[91]

$$\gamma(p) = 0.312 + (0.561/p) + (0.100/p^2) \quad (23)$$

Above $p > 10$ the limiting value ($\gamma = 0.386$) can be used.

From Eqs. 16 and 20 we can obtain an estimate for the rod length L if we know M or M_L (see above discussion) and have an estimate for the diameter d. As pointed out by Garcia de la Torre[92] the choice for d is not so critical since it comes into the equations as the logarithm. It applies only to those polysaccharides which are known to be rod like.

5.5. Semi-flexible chains: worm-like coils

Most linear polysaccharides are not rigid rods at all but are semi-flexible structures. The conformation and hydrodynamics of semi-flexible chains are most usefully represented by worm-like chains (see Refs. 93–96), in which the bending flexibility is represented by the persistence length L_p. This is an intrinsic property of a linear macromolecule: the greater the L_p the greater the rigidity and vice versa. More precisely, the conformation and flexibility of a macromolecular chain depends directly on L/L_p, the ratio of the contour length to the persistence length. For $L/L_p \ll 1$ the conformation is rod like and Eqs. 21–23 can be applied. For $L/L_p \gg 0$ the conformation approaches that of a random coil.[93–96] This can be best seen from the dependence of the radius of gyration on chain length, as clearly described by Freire and Garcia de la Torre:[96]

$$R_g^2 = \{L \cdot L_p/3\}.\{1 - (3L/L_p) + (6L_p^2/L^2)$$
$$+ 6(L_p^3/L^3)(1 - e^{-L/L_p})\} \quad (24)$$

In the limit $L_p/L \sim 0$, R_g is proportional to $L^{1/2}$ (n.b. this is misprinted in 96)—the classical dependence for a random coil—whereas when $L_p/L_o \gg 1$, the classical relation for a rod is obtained: $R_g = L/\sqrt{12}$.

The sedimentation coefficient for worm-like chains was first worked out by Hearst and Stockmayer,[97] later improved by Yamakawa and Fujii[98] to give this expression for s^o:

$$s^o = \{M(1 - \bar{v}\rho_o)/(3\pi\eta_o N_A L)\} \cdot \{1.843$$
$$\times \ln(L/2L_p)^{1/2} + \alpha_2 + \alpha_3 L/2L_p^{-1/2} + \cdots\} \quad (25)$$

If the persistence length L_p is much larger than the mean chain diameter, d, Yamakawa and Fujii gave limiting values for $\alpha_2 = -\ln(d/2L_p)$ and $\alpha_3 = 0.1382$. Freire and Garcia de la Torre[96] have further considered these coefficients. The factor $2L_p$ appears rather than L_p simply because $2L_p$ is equivalent to the statistical Kuhn segment length λ^{-1}.

A fundamental problem with the sedimentation coefficient is that it is the least sensitive parameter to conformation when compared with the intrinsic viscosity $[\eta]$ and the radius of gyration R_g. This lower sensitivity is offset by its ease of measurement and the ability to obtain s^o to a higher accuracy (to better than 1%) compared with the other parameters. Nonetheless it is advisable not to use s in isolation but in conjunction with R_g and $[\eta]$ versus M: two recent examples are a comparative study using ultracentrifugation, viscometry and light scattering on the relative conformations and flexibilities of galactomannans (guar, tara gum and locust bean gum), after pressure-assisted solubilisation procedures[35] and a study using ultracentrifugation, viscometry and small angle X-ray scattering to investigate the conformation and flexibility of heparin.[46]

6. Analysis of associative polysaccharide interactions

There are many instances where associative interactions involving polysaccharides, whether they be self-associa-

tion, complex formation or with small ligands are important. The analytical ultracentrifuge would appear to offer considerable potential for the analysis of these and other types of interaction. Indeed one of the main reasons behind the renaissance of analytical ultracentrifugation in the 1990s[99,100] was the simmering need by molecular biologists and protein chemists for noninvasive solution based methods for studying biomolecular interactions, particularly the weaker ones involved in molecular recognition phenomena (see, e.g., Refs. 101,102). The analytical ultracentrifuge—its clean, medium free (no columns or membranes)—and absolute nature has indeed proven a highly attractive tool for characterising the stoichiometry, reversibility and strength (as represented by the molar dissociation constant, K_d) of an interaction between well-defined systems: protein–protein, protein–DNA, protein–small ligand (see Refs. 1,2). With polysaccharides we are generally dealing with a different situation. Firstly a polysaccharide does not have a single, clearly defined molecular weight: it is polydisperse with a distribution of molecular weights. Secondly, weak interactions ($K_d > 50 \mu M$)—at least as far as we know—do not play a crucial functional role with polysaccharides as they do with proteins. Interactions, particularly involving polyelectrolytes of opposite charge (chitosan–alginate for encapsulation systems, chitosan–DNA for gene therapy) tend to be very strong or irreversible: the complexes tend to be much larger than for the simple associative protein–protein interactions. This means the main ultracentrifuge tool used for investigating protein–protein interactions, namely sedimentation equilibrium, has only limited applicability: sedimentation equilibrium has an upper limit of molecular weight of ∼50 million g/mol. Examples of the use of the analytical ultracentrifuge to assay interactions involving polysaccharides include a study on mixtures of alginate with bovine serum albumin[103,104] a study of galactomannan incubated with gliadin (as part of an ongoing investigation into the possible use of galactomannans to help intestinal problems)[105] chitosan with lysozyme[106] and synergistic interactions involving xanthan.[107] Polysaccharides can also regulate weak interactions between protein molecules. A recent example has been the use of the ultracentrifuge to study the effect of low molecular weight heparin molecules on the weak dimerisation of the plasminogen growth factor NK1, or at least a mutant thereof.[108] Rivas and co-workers have investigated the effect of nonspecific exclusion-volume or 'crowding' types of interaction of dextrans on the self-association tubulin.[109]

For large irreversible complexes involving polysaccharides a more valid assay procedure is to use sedimentation velocity (which can cope with complexes as large as 10^9 g/mol), with change in sedimentation coefficient (s, normalised to standard conditions or not) or as our

marker for complex formation. If we so wish we can then convert this to a change in molecular weight if we assume a conformation and use the power law relation Eq. 11. Alternatively we can simply use s directly as our size criterion (this is not unusual): it is used, for example, in ribosome size representations, 30S, 50S etc., or in seed globulin, the 7S, 11S soya bean globulins etc.[110]

6.1. Polysaccharide mucoadhesive interactions

A good example of where sedimentation velocity has played a valuable role in assaying large polysaccharide complexes is in the assessment of polysaccharides as mucoadhesives (see Refs. 112–114 and refs therein): a drug administered orally or nasally tends to be washed away from the site of maximum absorption by the bodies natural clearance mechanisms before being absorbed. Incorporating the drug into a polysaccharide material which interacts with epithelial mucus in a controllable way has been proposed as a method of increasing the residence time and enhancing the absorption rate. The key macromolecule in mucus is mucin glycoprotein—a linear polypeptide backbone—with linked saccharide chains to the extent that >80% of the molecule is carbohydrate.[50] The carbohydrate has potential sites for ionic interaction (clusters of sialic acid or sulfate residues) and also hydrophobic interaction (clusters of methyl groups offered by fucose residues). Sedimentation velocity has been a valuable tool in the selection of appropriate mucoadhesives and in the characterisation of the complexes.[112–117]

The approach is to first of all obtain mucin to a high degree of purity and to characterise the mucin and potential mucoadhesive. This is done by sedimentation velocity ($g^*(s)$ analysis), sedimentation equilibrium (M^* analysis)—according to the procedures described above, together with SEC-MALLs.[118,119] The reactants are then mixed in various proportions, and the sedimentation ratio ($s_{complex}/s_{mucin}$)—the ratio of the sedimentation coefficient of the complex to that of the pure mucin itself—is used as the measure for mucoadhesion. The ultraviolet absorption optics on the XL-A or XL-I ultracentrifuge have been used as the main optical detection system. Although the polysaccharide is generally invisible in the near UV (∼280 nm), at the concentrations normally employed, the mucin—in uncomplexed and complexed form—is detectable.

This procedure has been used to assay the mucoadhesive performance of a whole range of polysaccharides. Neutral and polyanionic species showed no interaction with mucin ($s_{complex}/s_{mucin} \approx 1$)[120,114,115,117] reinforcing macroscopic observations on whole mucus using tensiometry.[120] A contrasting picture is seen for chitosans. A highly charged chitosan ('sea cure' 210+) of degree of acetylation $F_A \sim 0.11$ has impressive sedimentation

ratios of 15–38 depending on the temperature. Interestingly for a lower-charged chitosan of $F_A \sim 0.42$, values of 31–44 were returned, reinforcing a view that both electrostatic and hydrophobic effects are important. The demonstration of large-size interaction products by the analytical ultracentrifuge used in this manner is reinforced by images from the powerful imaging techniques of electron microscopy and atomic force microscopy. Conventional transmission electron microscopy clearly demonstrates large complexes of the order of $\sim 1\ \mu m$ in size,[121] and if we label the chitosan with gold we can see that the chitosan is distributed throughout the complex with 'hot spots' in the interior.[113] Images from atomic force microscopy, visualised in topographic and phase modes, again shows complexes of this size. Control experiments revealed a loose coiled structure for pig gastric mucin and a shorter, stiffer conformation for the chitosan, consistent with solution measurements.[122] An advantage of the analytical ultracentrifuge is that since it is a pure solution technique with no columns or membranes it allows us to easily alter the surrounding solvent conditions. For example,[111,113] if we vary the pH we see that the sedimentation ratio is ~ 34–48 at pH ~ 6.5 but is still found to be significant at pH 2.0 ($s_{complex}/s_{mucin} \sim 12$–$22$), below the pK_a of the sialic acid groups on the mucin—which not only suggests the importance of the electrostatic contribution but indicate the existence of significant hydrophobic types of interaction. Attempts to investigate the effects of bile salts and differing ionic strengths down the alimentary tract also yield very much the same picture.[111,114] At 0 mM bile salt $s_{complex}/s_{mucin}$ was found to be ~ 18–21, whereas at 6 mM the interaction is still significant, with $s_{complex}/s_{mucin} \sim 14$–$18$.

6.2. Sedimentation fingerprinting

Much of the work on the molecular basis of mucoadhesion has involved mucin extracted from a source available in large quantities: pig gastric mucus. Researchers would dearly love to perform these types of experiments on human small intestinal mucin if it could be obtained in sufficient quantities in purified form. There has however been success in performing experiments on human mucin extracted from different parts of the stomach, namely the cardia, corpus and antrum regions. Although available in miniscule quantities we can assay mucoadhesiveness of chitosan on these by using a modification of the approach using the analytical ultracentrifuge described above, called Sedimentation Fingerprinting. In this method, introduced a few years ago,[123] the Schlieren optical system is used to record the concentration (refractive index) gradient dn/dr as a function of radial position r in the ultracentrifuge cell. The area under a 'Schlieren peak' provides a measure of the sedimenting concentration. Alternatively, if interference optics on the XL-I ultracentrifuge are used, the area under a $g^*(s)$ versus s or $c(s)$ versus s plot would provide similar concentration information. Although the mucins from human stomach are at too low a concentration to be detected we can assay for interaction from the loss of area under the chitosan peak caused by interaction. In this way it has been possible to show significant differences in mucoadhesive interactions for different regions of the stomach. This type of information obtained with the ultracentrifuge reinforced with other data is helping us design effective mucoadhesive systems. The current challenge is to design cross-linked chitosan encapsulation systems using, for example, tripolyphosphate:[124] in this regard the use of co-sedimentation strategies to assay for effective encapsulation of a drug—as successfully applied previously to synthetic polymer systems[125–127] will prove useful. This and other aspects are considered in a recent review specifically on mucoadhesion.[111]

7. Macromolecular charge and charge screening measurement

The final application which is providing us with a considerable challenge is the measurement of charge on polyelectrolyte polysaccharides, and the extent of charge screening through interaction with low molecular weight electrolyte.[128] In recent years there has been a tendency to identify the charges on polysaccharides (and polynucleotides) with the values calculated from the chemical structure. However, the phenomenon of charge screening (or counterion condensation) has long been an established feature of polyelectrolyte theory.[129–131] Winzor and co-workers have employed measurements of the Donnan distribution of small ions in dialysis[128] to reinforce earlier evidence of charge-screening effects in polysaccharide anions.[132,133] These researchers used the absorption optical system of a Beckman XL-I ultracentrifuge to monitor the distribution of ions in polysaccharide solutions dialysed against a buffered solution (pH 6.8, I 0.08) supplemented with 0.2 mM chromate as an indicator ion. After extensive dialysis against the same chromate-supplemented buffer to establish the Donnan equilibrium distribution of small ions, the difference between chromate concentrations in the polysaccharide and diffusate solutions was monitored by means of the absorption optical system: the ultracentrifuge is merely being used as a double-beam spectrophotometer when a sufficiently low speed (3000 rpm) is used to ensure uniformity of solution composition throughout the cell. As in classical difference spectroscopy, diffusate was placed in the reference sector of the cell to allow direct measurement of the absorbance difference from a scan at 375 nm.

For dextran sulfate, heparin and polygalacturonate, the effective net charges were shown by these researchers to be only one-third of those deduced from the chemical structures[128]—a reflection of charge screening (counter-ion condensation) in aqueous polyelectrolyte solutions. Whereas the extent of charge screening for the first two polysaccharides agrees well with theoretical prediction, the disparity in the corresponding comparison for polygalacturonate was deemed to reflect partial esterification of carboxyl groups, whereupon the experimental parameter refers to the effective charge per hexose residue rather than the effective fractional charge of each carboxyl group. The use of the ultracentrifuge in this way appears to have shown it is therefore wrong to calculate the charge on a polysaccharide in solution on the basis merely on the numbers or number density of charged residues like CO_2^- or SO_3^{2-}, even in cases where the pH is such that the groups are fully ionised.

8. Concluding remarks

It is hoped this short review has demonstrated that, whilst there are still challenges to be met, the analytical ultracentrifuge can form a useful part of the armoury of methods available to a researcher interested in understanding the size, conformation modelling and interaction properties of polysaccharides in the environment where many occur naturally—in solution state. The challenges have been made easier since neither sedimentation velocity nor sedimentation equilibrium require the need for columns or membranes or immobilisation onto a surface: it is a free solution technique.

In several places in this review of the use and potential use of the ultracentrifuge we have referred tangentially to comparable results obtained via light scattering. Certainly sedimentation velocity and SEC-MALLS can provide complementary information on the heterogeneity of material. Unlike SEC-MALLS the former provides a sedimentation coefficient as opposed to a molecular weight distribution although no column or separation medium is required and hence no worries concerning column/medium inertness. It is our opinion that in a characterisation of a polysaccharide solution *both* methods should be used. For conformation analysis the two corresponding principal parameters—the sedimentation coefficient and the radius of gyration, again provide complementary information, and as we have seen for the analysis of polysaccharide interactions and complex formation—and the particular case of mucoadhesion-the two techniques again providing complementary information.

It is also worth pointing out that this article, in focussing on solutions, has not considered the opportunities it also provides for the analysis of the rheological and thermodynamic properties of polysaccharide gels,[134]

phase diffusion and interfacial transport phenomena involving polysaccharides,[135] and the formation of films and membranes.[136] For solution work the main challenges appear to be in providing better representations of sedimentation coefficient distributions. With conformation modelling studies the ease of measurement of the sedimentation coefficient is countered by its lower sensitivity compared to the radius of gyration and intrinsic viscosity: development of global procedures involving s, R_g and $[\eta]$ and their dependencies on molecular weight would appear a useful way forward, and efforts are now well underway to address this.

References

1. Harding, S. E.; Winzor, D. J. Sedimentation velocity in the analytical ultracentrifuge. In *Protein–Ligand Interactions: Hydrodynamics and Calorimetry*; Harding, S. E., Chowdhry, B. Z., Eds.; Oxford University Press: United Kingdom, 2001; pp 75–103.
2. Winzor, D. J.; Harding, S. E. Sedimentation equilibrium in the analytical ultracentrifuge. In *Protein–Ligand Interactions: Hydrodynamics and Calorimetry*; Harding, S. E., Chowdhry, B. Z., Eds.; Oxford University Press: United Kingdom, 2001; pp 105–135.
3. Tombs, M. P.; Harding, S. E. *An Introduction to Polysaccharide Biotechnology*; Taylor and Francis: London, 1997.
4. Lapasin, R.; Pricl, S. *Rheology of Industrial Polysaccharides. Theory and Applications*; Blackie: London, United Kingdom, 1995.
5. *Analytical Ultracentrifugation in Biochemistry and Polymer Science*; Harding, S. E., Rowe, A. J., Horton, J. C., Eds.; Royal Society of Chemistry: Cambridge, United Kingdom, 1992.
6. Gregurik, S. K.; Liu, J. H.-Y.; Brant, D. A. *J. Phys. Chem. B* **1999**, *103*, 3476–3488.
7. McIntire, T. M.; Brant, D. A. *Int. J. Biol. Macromol.* **1999**, *26*, 303–310.
8. Perico, A.; Mormino, M.; Urbani, R.; Cesaro, A.; Tylianakis, E.; Dais, P.; Brant, D. A. *J. Phys. Chem. B* **1999**, *103*, 8162–8171.
9. Liu, J. H.-Y.; Brant, D. A.; Kitamura, S.; Kajiwara, K.; Mimura, M. *Macromolecules* **1999**, *32*, 8611–8620.
10. Brant, D. A. *Curr. Opin. Struct. Biol.* **1999**, *9*, 556–562.
11. Liu, J. H.-Y.; Brameld, K. A.; Brant, D. A.; Goddard, W. A., III. *Polymer* **2002**, *43*, 509–516.
12. Furst, A. J. *Europ. Biophys. J.* **1997**, *25*, 307–310.
13. Theisen, C.; Johann, C.; Deacon, M. P.; Harding, S. E. *Refractive Increment Data Book for Polymer and Biomolecular Scientists*; Nottingham University Press: United Kingdom, 2000.
14. Anthonsen, M. W.; Vårum, K. M.; Smidsrød, O. *Carbohydr. Polym.* **1993**, *22*, 193–201.
15. Preston, B. N.; Wik, K. O. In *Analytical Ultracentrifugation in Biochemistry and Polymer Science*; Harding, S.

E., Rowe, A. J., Horton, J. C., Eds.; Royal Society of Chemistry: Cambridge, 1992; pp 549–567.

16. Schachman, H. *Ultracentrifugation in Biochemistry*; Academic: New York, 1959.

17. Gibbons, R. A. In *Glycoproteins: Their Composition, Structure and Function*; Gottschalk, A., Ed.; Elsevier: Amsterdam, 1972; Vol. 5, Part A, pp 128–140.

18. Kratky, O.; Leopold, H.; Stabinger, H. *Meth. Enzymol.* **1973**, *27D*, 98–110.

19. Laue, T. M.; Shah, B. D.; Ridgeway, T. M.; Pelletier, S. L. In *Analytical Ultracentrifugation in Biochemistry and Polymer Science*; Harding, S. E., Rowe, A. J., Horton, J. C., Eds.; Royal Society of Chemistry: Cambridge, United Kingdom, 1992; pp 90–125.

20. http://www.jphilo.mailway.com/download.htm and http://www.rasmb.bbri.org/rasmb/windows/sednterp-philo/.

21. Gralén, N. *Sedimentation and Diffusion Measurements on Cellulose and Cellulose Derivatives*, PhD Dissertation, University of Uppsala, Sweden, 1944.

22. Rowe, A. J. *Biopolymers* **1977**, *16*, 2595–2611.

23. Rowe, A. J. In *Analytical Ultracentrifugation in Biochemistry and Polymer Science*; Harding, S. E., Rowe, A. J., Horton, J. C., Eds.; Royal Society of Chemistry: Cambridge, United Kingdom, 1992; pp 359–393.

24. Fujita, H. *Mathematical Theory of Sedimentation Analysis*; New York, USA: Academic, 1962.

25. Fujita, H. *Foundations of Ultracentrifugal Analysis*; Wiley: New York, USA, 1975.

26. Majzoobi, M. *The Effect of Processing on the Molecular Structure of Wheat Starch*, PhD Dissertation, University of Nottingham, United Kingdom, 2004.

27. Stafford, W. In *Analytical Ultracentrifugation in Biochemistry and Polymer Science*; Harding, S. E., Rowe, A. J., Horton, J. C., Eds.; Royal Society of Chemistry: Cambridge, United Kingdom, 1992; pp 359–393.

28. Philo, J. S. *Anal. Biochem.* **2000**, *279*, 151–163.

29. Schuck, P. *Biophys. J.* **1998**, *75*, 1503–1512.

30. Dam, J.; Schuck, P. *Methods Enzymol.* **2003**, *384*, 121–185.

31. Lamm, O. *Ark. Mat. Astr. Fys.* **1929**, *21B*(2), 1–4.

32. Claverie, J. M.; Dreux, H.; Cohen, R. *Biopolymers* **1975**, *14*, 1685–1700.

33. http://www.analyticalultracentrifugation.com/download.htm.

34. Harding, S. E. *Biophys. Chem.* **1995**, *55*, 69–93.

35. Harding, S. E.; Ross-Murphy, S. B.; Patel, T.; Picout, D. R.; Garcia de la Torre, J. (in preparation).

36. Svedberg, T.; Pedersen, K. O. *The Ultracentrifuge*; Oxford University Press: United Kingdom, 1940.

37. Korneeva, E. V.; Vichoreva, G. A.; Harding, S. E.; Pavlov, G. M. *Abstr. Am. Chem. Soc.* **1996**, *212*, 75-cell.

38. Pavlov, G. M.; Korneeva, E. V.; Harding, S. E.; Vichoreva, G. A. *Polymer* **1998**, *39*, 6951–6961.

39. Burchard, W. In *Laser Light Scattering in Biochemistry*; Harding, S. E., Sattelle, D. B., Bloomfield, V. A., Eds.; Royal Society of Chemistry: Cambridge, United Kingdom, 1992; pp 3–22.

40. Pavlov, G. M.; Korneeva, E. V.; Nepogod'ev, S. A.; Jumel, K.; Harding, S. E. *Polym. Sci. Ser. A* **1998**, *40*, 1282–1289; *Vysokomolekulyarnye Soed. Ser. A* **1998**, *40*, 2056–2064.

41. Pavlov, G. M.; Korneeva, E. V.; Jumel, K.; Harding, S. E.; Meyer, E. W.; Peerlings, H. W. I.; Stoddart, J. F.; Nepogodiev, S. A. *Carbohydr. Polym.* **1999**, *38*, 195–202.

42. Sharman, W. R.; Richards, E. L.; Malcolm, G. N. *Biopolymers* **1978**, *17*, 2817–2833.

43. Igarishi, O.; Sakurai, Y. *Agric. Biol. Chem.* **1965**, *29*, 678.

44. Djurtoft, R.; Rasmussen, K. L. *Eur. Brew. Conv. Congress* **1955**, 17.

45. Wedlock, D. J.; Fasihuddin, B. A.; Phillips, G. O. *Int. J. Biol. Macromol.* **1986**, *8*, 57–61.

46. Pavlov, G.; Finet, S.; Tatarenko, K.; Korneeva, E.; Ebel, C. *Eur. Biophys. J.* **2003**, *32*, 437–449.

47. Pusey, P. N. In *Photon Correlation and Light Beating Spectroscopy*; Cummings, H. Z., Pike, E. R., Eds.; Plenum: New York, USA, 1974; pp 387–428.

48. Smidsrød, O.; Andresen, I. L. *Biopolymerkjemi*; Tapir: Trondheim, Norway, 1979.

49. Tsvetkov, V. N.; Eskin, V.; Frenkel, S. *Structure of Macromolecules in Solution*; Butterworths: London 1970.

50. Harding, S. E. *Adv. Carbohydr. Chem. Biochem.* **1989**, *47*, 345–381.

51. Pain, R. H. *Symp. Soc. Exp. Biol.* **1980**, *34*, 359–376.

52. Svedberg, T.; Fåhraeus, R. *J. Am. Chem. Soc.* **1926**, *48*, 430–438.

53. http://www.wyatt.com/.

54. Horton, J. C.; Harding, S. E.; Mitchell, J. R. *Biochem. Soc. Trans.* **1991**, *19*, 510–511.

55. Rollings, J. E. *Biochem. Soc. Trans.* **1991**, *19*, 493.

56. Rollings, J. E. In *Laser Light Scattering in Biochemistry*; Harding, S. E., Sattelle, D. B., Bloomfield, V. A., Eds.; Royal Society of Chemistry: Cambridge, United Kingdom, 1992; pp 275–293.

57. Wolff, D.; Czapla, S.; Heyer, A. G.; Radosta, S.; Mischnick, P.; Springer, J. *Polymer* **2000**, *41*, 8009–8016.

58. Auzeály, R.; Rinaudo, M. *Macromol. Biosci.* **2003**, *3*, 562–565.

59. Clewlow, A. C.; Errington, N.; Rowe, A. J. *Eur. Biophys. J.* **1997**, *25*, 311–318.

60. Mächtle, W. *Prog. Colloid Polym. Sci.* **1999**, *113*, 1–9.

61. Creeth, J. M.; Harding, S. E. *Biochem. J.* **1982**, *205*, 639–641.

62. Harding, S. E. In *Analytical Ultracentrifugation in Biochemistry and Polymer Science*; Harding, S. E., Rowe, A. J., Horton, J. C., Eds.; Royal Society of Chemistry: Cambridge, United Kingdom, 1992; pp 495–516.

63. Harding, S. E. *Gums Stabilis. Food Ind.* **1993**, *8*, 55–65.

64. Harding, S. E.; Horton, J. C.; Morgan, P. J. In *Analytical Ultracentrifugation in Biochemistry and Polymer Science*; Harding, S. E., Rowe, A. J., Horton, J. C., Eds.; Royal Society of Chemistry: Cambridge, United Kingdom, 1992; pp 275–294.

65. Cölfen, H.; Harding, S. E. *Eur. Biophys. J.* **1997**, *24*, 333–346.

66. Hall, D. R.; Harding, S. E.; Winzor, D. J. *Prog. Colloid Polym. Sci.* **1999**, *113*, 62–68.

67. Creeth, J. M.; Harding, S. E. *J. Biochem. Biophys. Meth.* **1982**, *7*, 25–34.

68. http://www.nottingham.ac.uk/ncmh/unit/method.html#Software.

69. Fee, M. *Evaluation of Chitosan Stability in Aqueous Systems*. PhD Dissertation, University of Nottingham, United Kingdom, 2004.

70. http://vm.uconn.edu/~wwwbiotc/uaf.html.

71. Creeth, J. M.; Pain, R. H. *Prog. Biophys. Mol. Biol.* **1967**, *17*, 217–287.

72. Yphantis, D. A. *Biochemistry* **1964**, *3*, 297–317.

73. Harding, S. E.; Day, K.; Dhami, R.; Lowe, P. M. *Carbohydr. Polym.* **1997**, *32*, 81–87.

74. Horton, J. C.; Harding, S. E.; Mitchell, J. R.; Morton-Holmes, D. F. *Food Hydrocolloids* **1991**, *5*, 125–127.
75. Stratmann, A.; Borchard, W. *Prog. Colloid Polym. Sci.* **2002**, *119*, 64–69.
76. Harding, S. E. *Biophys. J.* **1985**, *47*, 247–250.
77. Ball, A.; Harding, S. E.; Mitchell, J. R. *Int. J. Biol. Macromol.* **1988**, *10*, 259–264.
78. Harding, S. E.; Berth, G.; Ball, A.; Mitchell, J. R.; Garcia de la Torre, J. *Carbohydr. Polym.* **1991**, *16*, 1–15.
79. Wales, M.; Van Holde, K. E. *J. Polym. Sci.* **1954**, *14*, 81–86.
80. Creeth, J. M.; Knight, C. G. *Biochim. Biophys. Acta* **1965**, *102*, 549–558.
81. Lavrenko, P. N.; Linow, K. J.; Görnitz, E. In *Analytical Ultracentrifugation in Biochemistry and Polymer Science*; Harding, S. E., Rowe, A. J., Horton, J. C., Eds.; Royal Society of Chemistry: Cambridge, United Kingdom, 1992; pp 517–531.
82. Freed, K. F. *J. Chem. Phys.* **1976**, *65*, 4103–4110.
83. Kawahara, K.; Ohta, K.; Miyamoto, H.; Nakamura, S. *Carbohydr. Polym.* **1984**, *4*, 335–356.
84. Berth, G.; Cölfen, H.; Dautzenberg, H. *Prog. Colloid Polym. Sci.* **2002**, *119*, 50–57.
85. Harding, S. E.; Vårum, K. M.; Stokke, B. T.; Smidsrød, O. *Adv. Carbohydr. Anal.* **1991**, *1*, 63–144.
86. Pavlov, G. M. *Prog. Colloid Polym. Sci.* **2002**, *119*, 149–158.
87. Pavlov, G. M.; Rowe, A. J.; Harding, S. E. *Trends Anal. Chem.* **1997**, *16*, 401–405; Pavlov, G. M.; Harding, S. E.; Rowe, A. J. *Prog. Colloid Int. Sci.* **1999**, *113*, 76–80.
88. Stokke, B. T.; Elgsaeter, A. *Adv. Carbohydr. Anal.* **1991**, *1*, 195–247.
89. Harding, S. E.; Berth, G.; Hartmann, J.; Jumel, K.; Cölfen, H.; Christensen, B. E. *Biopolymers* **1996**, *39*, 729–736.
90. Broersma, S. *J. Chem. Phys.* **1960**, *32*, 1626–1635.
91. Tirado, M. M.; Garcia de la Torre, J. *J. Chem. Phys.* **1979**, *71*, 2581–2587.
92. Garcia de la Torre, J. In *Analytical Ultracentrifugation in Biochemistry and Polymer Science*; Harding, S. E., Rowe, A. J., Horton, J. C., Eds.; Royal Society of Chemistry: Cambridge, United Kingdom, 1992; pp 333–345.
93. Yamakawa, H. *Modern Theory of Polymer Solutions*; Harper and Row: New York, USA, 1971.
94. Bloomfield, V. A.; Crothers, D. M.; Tinoco, L. *Physical Chemistry of Nucleic Acids*; Harper and Row: New York, USA, 1974.
95. Cantor, C. R.; Schimmel, P. R. *Biophysical Chemistry*; Freeman: New York, USA, 1979.
96. Freire, J. J.; Garcia de la Torre, J. In *Analytical Ultracentrifugation in Biochemistry and Polymer Science*; Harding, S. E., Rowe, A. J., Horton, J. C., Eds.; Royal Society of Chemistry: Cambridge, United Kingdom, 1992; pp 346–358.
97. Hearst, J. E.; Stockmayer, W. H. *J. Chem. Phys.* **1962**, *37*, 1425–1433.
98. Yamakawa, H.; Fujii, M. *Macromolecules* **1973**, *6*, 407–415.
99. Schachman, H. K. *Nature* **1989**, *941*, 259.
100. Schachman, H. K. In *Analytical Ultracentrifugation in Biochemistry and Polymer Science*; Harding, S. E., Rowe, A. J., Horton, J. C., Eds.; Royal Society of Chemistry: Cambridge, 1992; pp 3–15.
101. Watson, J. D. *The Molecular Biology of the Gene*, 2nd ed.; Benjamin: New York, 1970.
102. Silkowski, H.; Davis, S. J.; Barclay, A. N.; Rowe, A. J.; Harding, S. E.; Byron, O. *Eur. Biophys. J.* **1997**, *25*, 455–462.
103. Harding, S. E.; Jumel, K.; Kelly, R.; Gudo, E.; Horton, J. C.; Mitchell, J. R. In *Food Proteins: Structure and Functionality*; Schwenke, K. D., Mothes, R., Eds.; VCH Verlagsgesellschaft: Weinheim, Germany, 1993; pp 216–226.
104. Kelly, R.; Gudo, E. S.; Mitchell, J. R.; Harding, S. E. *Carbohydr. Polym.* **1994**, *23*, 115–120.
105. Seifert, A.; Heinevetter, L.; Cölfen, H.; Harding, S. E. *Carbohydr. Polym.* **1995**, *28*, 325–332.
106. Cölfen, H.; Harding, S. E.; Vårum, K. M.; Winzor, D. J. *Carbohydr. Polym.* **1996**, *30*, 45–53.
107. Mannion, R. O.; Melia, C. D.; Launay, B.; Cuvelier, G.; Hill, S. E.; Harding, S. E.; Mitchell, J. R. *Carbohydr. Polym.* **1992**, *19*, 91–97.
108. Bandyopadhyay, A. *Structural Biology of the Plasminogen-related Growth Factors and their Receptors*, PhD thesis, University of Cambridge: Cambridge, United Kingdom, 2004.
109. Rivas, G.; Fernandez, J. A.; Minton, A. P. *Biochemistry* **1999**, *38*, 9379–9388.
110. Schwenke, K. D. *Eiweißquellen der Zukunft*; Urania: Leipzig, German Democratic Republic, 1985.
111. Harding, S. E. *Biochem. Soc. Trans.* **2003**, *31*, 1036–1041.
112. Deacon, M. P. *Polymer Bioadhesives for Drug Delivery*. PhD Dissertation, University of Nottingham, United Kingdom, 1999.
113. Fiebrig, I.; Vårum, K. M.; Harding, S. E.; Davis, S. S.; Stokke, B. T. *Carbohydr. Polym.* **1997**, *33*, 91–99.
114. Harding, S. E.; Deacon, M. P.; Fiebrig, I.; Davis, S. S. *Biotech. Gen. Eng. Rev.* **1999**, *16*, 41–86.
115. Fiebrig, I.; Davis, S. S.; Harding, S. E. In *Biopolymer Mixtures*; Harding, S. E., Hill, S. E., Mitchell, J. R., Eds.; Nottingham University Press: United Kingdom, 1995; pp 373–419.
116. Fiebrig, I. *Solution Studies on the Mucoadhesive Potential of Various Polymers for use in Gastrointestinal Drug Delivery Systems*. PhD Dissertation, University of Nottingham, United Kingdom, 1995.
117. Anderson, M. T.; Harding, S. E.; Davis, S. S. *Biochem. Soc. Trans.* **1989**, *17*, 1101–1102.
118. Fiebrig, I.; Harding, S. E.; Davis, S. S. *Prog. Colloid Polym. Sci.* **1994**, *94*, 66–73.
119. Jumel, K.; Fogg, F. J. J.; Hutton, D. A.; Pearson, J. P.; Allen, A.; Harding, S. E. *Eur. Biophys. J.* **1997**, *25*, 477–480.
120. Lehr, C. M.; Bouwstra, J. A.; Schacht, E. H.; Junginger, H. E. *Int. J. Pharmaceut.* **1992**, *78*, 43–48.
121. Fiebrig, I.; Harding, S. E.; Rowe, A. J.; Hyman, S. C.; Davis, S. S. *Carbohydr. Polym.* **1995**, *28*, 239–244.
122. Deacon, M. P.; McGurk, S.; Roberts, C. J.; Williams, P. M.; Tendler, S. J. B.; Davies, M. C.; Davis, S. S.; Harding, S. E. *Biochem. J.* **2000**, *348*, 557–563.
123. Deacon, M. P.; Davis, S. S.; White, R. J.; Nordman, H.; Carlstedt, I.; Errington, N.; Rowe, A. J.; Harding, S. E. *Carbohydr. Polym.* **1999**, *38*, 235–238.
124. Zengshuan, M. A.; Yeoh, H. H.; Lim, L. Y. *J. Pharm Sci.* **2002**, *91*, 1396–1404.
125. Morgan, P. J.; Harding, S. E.; Petrak, K. *Macromolecules* **1990**, *23*, 4461–4464.
126. Davison, C. J.; Smith, K. E.; Hutchinson, L. E. F.; O'Mullane, J. E.; Harding, S. E.; Brookman, L.; Petrak, K. *J. Bioact. Compat. Polym.* **1990**, *5*, 267–283.

127. Hagan, S. A.; Coombes, A. G. A.; Garnett, M. C.; Dunn, S. E.; Davies, M. C.; Illum, I.; Davis, S. S.; Harding, S. E.; Purkiss, S.; Gellert, P. R. *Langmuir* **1996**, *12*, 2153–2161.
128. Winzor, D. J.; Carrington, L. E.; Deszczynski, M.; Harding, S. E. *Biomacromolecules* **2004**, *5*, 2456–2460.
129. Katchalsky, A.; Alexandrowicz, Z.; Kedem, O. In *Chemical Physics of Ionic Solutions*; Conway, B. E., Barradas, R. G., Eds.; Wiley: New York, USA, 1996; pp 295–346.
130. Manning, G. S. *J. Chem. Phys.* **1969**, *51*, 924–931.
131. Manning, G. S. *Q. Rev. Biophys.* **1978**, *11*, 179–246.
132. Adair, G. S.; Adair, M. E. *Biochem. J.* **1934**, *28*, 199.
133. Svensson, H. *Ark. Kemi Mineral. Geol.* **1946**, *22A*(10), 1.
134. Cölfen, H. *Biotech. Genet. Eng. Rev.* **1999**, *16*, 87–140.
135. Harding, S. E.; Tombs, M. P. *Biotechnol. Genet. Eng. Rev.* **2002**, *19*, 55–69.
136. Wandrey, C.; Grigorescu, G.; Hunkeler, D. *Prog. Colloid Polym. Sci.* **2002**, *119*, 84–91.